J|A|C|S
ARTICLES
Published on Web 12/13/2001

Polyunsaturated Fatty Acids in Lipid Bilayers: Intrinsic and Environmental Contributions to Their Unique Physical Properties

Scott E. Feller,*,† Klaus Gawrisch,‡ and Alexander D. MacKerell, Jr.*,§

Contribution from the Department of Chemistry, Wabash College, Crawfordsville, Indiana 47933, Laboratory of Membrane Biochemistry and Biophysics, NIAAA, National Institutes of Health, Rockville, Maryland 20852, and Department of Pharmaceutical Sciences, School of Pharmacy, University of Maryland, Baltimore, Maryland 21201

Received July 27, 2001

Abstract: Polyunsaturated lipids are an essential component of biological membranes, influencing order and dynamics of lipids, protein−lipid interaction, and membrane transport properties. To gain an atomic level picture of the impact of polyunsaturation on membrane properties, quantum mechanical (QM) and empirical force field based calculations have been undertaken. The QM calculations of the torsional energy surface for rotation about vinyl−methylene bonds reveal low barriers to rotation, indicating an intrinsic propensity toward flexibility. Based on QM and experimental data, empirical force field parameters were developed for polyunsaturated lipids and applied in a 16 ns molecular dynamics (MD) simulation of a 1-stearoyl-2-docosahexaenoyl-*sn*-glyerco-3-phosphocholine (SDPC) lipid bilayer. The simulation results are in good agreement with experimental data, suggesting an unusually high degree of conformational flexibility of polyunsaturated hydrocarbon chains in membranes. The detailed analysis of chain conformation and dynamics by simulations is aiding the interpretation of experimental data and is useful for understanding the unique role of polyunsaturated lipids in biological membranes. The complete force field is included as Supporting Information and is available from http://www.pharmacy.umaryland.edu/faculty/amackere/research.html.

Introduction

Cell membranes from the nervous system are known to contain high concentrations of polyunsaturated docosahexaenoic acid (DHA), a fatty acid with 22 carbons and 6 double bonds (Figure 1). Recent evidence suggests that high DHA concentrations are critical for the function of G-protein coupled membrane receptors such as rhodopsin.[1] The structure and dynamics of these polyunsaturated chains within membranes is largely unknown. The six cis-double bonds may reduce the chain flexibility because of the smaller number of rotatable carbon−carbon bonds. However, recent NMR and X-ray scattering measurements suggest that the polyunsaturated chains are far more compressible laterally than their saturated counterparts,[2] and that the chains are undergoing rapid conformational transitions between a diverse group of states.[3] Additionally, the rate of water permeation across the bilayer is observed to increase dramatically with polyunsaturation.[4,5] The many interesting questions suggested by these experiments and numerous others[6−12] motivated us to undertake a theoretical study of this important class of lipids.

Theoretical methods for the investigation of biological molecules are now ubiquitous in biochemistry and biophysics.[13] These approaches allow for detailed atomic models of biological systems to be obtained, from which structure−function relationships can be elucidated. In particular, quantum mechanical (QM) methods allow for detailed studies of the structure and energetics of small molecules representative of biomolecules to be investigated. Recent examples from our laboratories include studies on nucleic acid components and lipid fragments.[14,15] Complementary methods based on empirical force fields,

* Address correspondence to this author.
† Wabash College: (telephone) 765-361-6175; (fax) 765-361-6340; (e-mail) fellers@wabash.edu.
‡ National Institutes of Health.
§ University of Maryland: (telephone) 410-706-7442; (fax) 410-706-0346; (e-mail) alex@outerbanks.umaryland.edu.

(1) Mitchell, D. C.; Gawrisch, K.; Litman, B. J.; Salem, N. *Biochem. Soc. Trans.* **1998**, *26*, 365−370.
(2) Koenig, B. W.; Strey, H. H.; Gawrisch, K. *Biophys. J.* **1997**, *73*, 1954−1966.
(3) Holte, L. L.; Koenig, B. W.; Gawrisch, K. *Biochemistry*. Submitted for publication.
(4) Olbrich K. C.; Rawicz, W.; Needham, D.; Evans, E. *Biophys. J.* **2000**, *79*, 321−327.
(5) Huster, D.; Jin, A. J.; Arnold, K.; Gawrisch, K. *Biophys. J.* **1997**, *73*, 855−864.
(6) Holte L. L.; Gawrisch, K. *Biochemistry* **1997**, *36*, 4669.
(7) Huster, D.; Arnold, K.; Gawrisch K. *Biochemistry* **1998**, *37*, 17299.
(8) Safley, A. M.; Polozov, I. V.; Gawrisch, K. *Biophys. J.* **2000**, *78*, 412.
(9) Dratz, E. A.; Deese, A. J. In *Health Effects of Polyunsaturated Fatty Acids in Seafoods*; Simopolous, A. P., Kifer, R. R., Martin, R. E., Eds.; Academic Press: New York, 1986; pp 319−51.
(10) Baenziger, J. E.; Jarrell, H. C.; Smith, I. C. *Biochemistry* **1992**, *31*, 3377.
(11) Rajamoorthi, K.; Brown, M. F. *Biochemistry* **1991**, *30*, 4204.
(12) Everts, S.; Davis, J. H. *Biophys. J.* **2000**, 79, 885−897.
(13) Becker, O. M.; MacKerell, A. D.; Roux, B.; Watanabe, M. *Computational Biochemistry and Biophysics*; Marcel-Dekker: New York, 2001.
(14) Banavali, N. K.; MacKerell, A. D., Jr. *J. Am. Chem. Soc.* **2001**, In Press.
(15) Foloppe, N.; Nilsson, L.; MacKerell, A. D. J. *Biopolymers*. Submitted for publication.

10.1021/ja0118340 CCC: $22.00

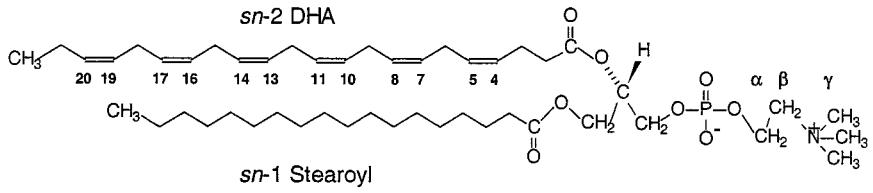

Figure 1. Structure of SDPC.

including molecular dynamics (MD) simulations, allow for calculations on complete biomolecules and assemblies of biomolecules in their aqueous environment. These large-scale MD simulations are especially important for the study of membrane components,[16] such as DHA, where intermolecular forces play a dominating role in organizing the system. MD simulations of lipid bilayer membranes have found use in providing information that is complementary to laboratory experiments and useful in the interpretation of diffraction[17] and NMR[18] data, and in providing a detailed picture of the membrane with extremely high spatial and temporal resolution.

There are many details that must be considered in carrying out such computer simulations, such as the time and length scale of the processes under study,[19,20] the statistical mechanical ensemble to be employed,[21] the algorithm used to integrate the equations of motion,[22] and the form of the energy function and its parametrization.[23] In the following we describe a combined QM and MD investigation of polyunsaturated lipids. The QM techniques are applied to model compounds to understand the intrinsic energetics of conformational transitions in polyunsaturated aliphatic chains. The results are then used to parametrize an empirical force field for hydrocarbon chains containing multiple sites of unsaturation separated by methylene groups. This is followed by a description of our simulation results for a 1-stearoyl-2-docosahexaenoyl-*sn*-glycero-3-phosphocholine (SDPC) bilayer and a comparison of these results with the available experimental data.

Methods

Quantum Mechanical Calculations. QM calculations were performed with the Gaussian 98 package[24] on the model compounds shown in Figure 2. In calculations on compound **D** the double bonds were always in the cis orientation (i.e. C−C=C−C = 0.0°), unless indicated otherwise. All calculations used the 6-31G** basis at the Hartree−Fock level or with second-order Møller−Plesset (MP2) perturbation[25] used to treat electron correlation. All optimizations were performed to default tolerances by using the level of theory stated in the text and figure legends (i.e. MP2 data were all optimized with MP2 to treat electron correlation). In the optimizations all degrees of freedom were allowed to relax except specific dihedrals as described below. Vibrational frequencies were calculated analytically. Determination of the potential energy distributions of the vibrational spectra was performed with the MOLVIB[26] module in the program CHARMM.

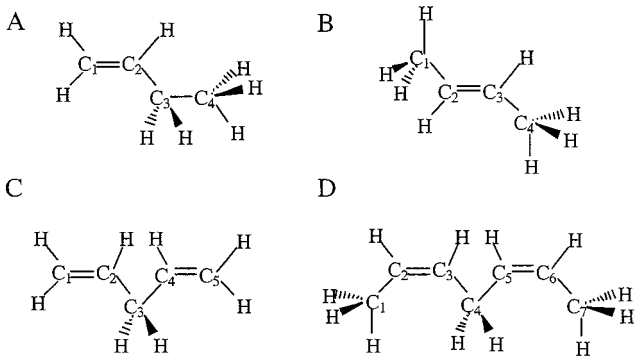

Figure 2. Model compounds used in the parameter optimization: (A) 1-butene, (B) 2-butene, (C) 1,4-pentadiene, and (D) 2,5-heptadiene.

Empirical Force Field Calculations. The program CHARMM (Chemistry at HARvard Molecular Mechanics)[23,27] was employed for empirical force field calculations. For the model compound calculations no truncation of the van der Waals or Coulombic interactions was performed. Energy minimizations were performed with the Adopted-Basis Newton Raphson (ABNR) minimizer followed by the Newton Raphson method to a root-mean-squared gradient of less than 10^{-6} kcal/mol/Å. When required, harmonic constraints of 10 000 kcal/mol/rad were used to fix selected dihedrals to the desired geometry. Vibrational spectra were calculated with the VIBRAN module in CHARMM with the potential energy distributions calculated with MOLVIB.[26]

Molecular Dynamics Simulation. The simulation protocol employed has been successfully applied to the simulation of numerous saturated and unsaturated phosphatidylcholine bilayers in the recent past[18,28−31] and is described here for completeness. The periodic simulation cell contained 72 lipids (36 per monolayer) and 15.1 water molecules/lipid, corresponding to the hydration state of samples prepared for X-ray and NMR investigations. A partially flexible simulation cell was employed with the z dimension (i.e., the bilayer normal) adjusted to maintain the $P_{zz} = 1$ atm, and the x and y dimensions were fixed to maintain a surface area of 65 Å^2/molecule,

(16) Feller, S. E. *Curr. Opin. Colloid Interface Sci.* **2000**, *5*, 217−223.
(17) Petrache, H. I.; Feller, S. E.; Nagle, J. F. *Biophys. J.* **1997**, *72*, 2237−2242.
(18) Feller, S. E.; Huster, D.; Gawrisch, K. *J. Am. Chem. Soc.* **1999**, *121*, 8963−8964.
(19) Pastor, R. W.; Feller, S. E. In *Biological Membranes: A Molecular Perspective from Computation and Experiment*; Merz, K. M., Roux, B., Eds.; Birkhauser: Boston, 1996; pp 3−30.
(20) Feller, S. E.; Pastor, R. W. *Biophys. J.* **1996**. *71*, 1350−1355.
(21) Zhang, Y.; Feller, S. E.; Brooks, B. R.; Pastor, R. W. *J. Chem. Phys.* **1995**, *103*, 10252−10266.
(22) Martyna, G. J.; Tobias, D. J.; Klein, M. L. *J. Chem. Phys.* **1994**, *101*, 4177−4199.
(23) MacKerell, A. D., Jr.; Brooks, B.; Brooks, C. L., III; Nilsson, L.; Roux, B.; Won, Y.; Karplus, M. In *Encyclopedia of Computational Chemistry*; Schleyer, P. v. R.; Allinger, N. L.; Clark, T.; Gasteiger, J.; Kollman, P. A., Schaefer, H. F., III, Schreiner, P. R., Eds.; John Wiley & Sons: Chichester, 1998; Vol. 1, pp 271−277.
(24) Frisch, M. J.; Trucks, G. W.; Schlegel, H. B.; Scuseria, G. E.; Robb, M. A.; Cheeseman, J. R.; Zakrzewski, V. G.; Montgomery, J. A., Jr.; Stratmann, R. E.; Burant, J. C.; Dapprich, S.; Millam, J. M.; Daniels, A. D.; Kudin, K. N.; Strain, M. C.; Farkas, O.; Tomasi, J.; Barone, V.; Cossi, M.; Cammi, R.; Mennucci, B.; Pomelli, C.; Adamo, C.; Clifford, S.; Ochterski, J.; Petersson, G. A.; Ayala, P. Y.; Cui, Q.; Morokuma, K.; Malick, D. K.; Rabuck, A. D.; Raghavachari, K.; Foresman, J. B.; Cioslowski, J.; Ortiz, J. V.; Baboul, A. G.; Stefanov, B. B.; Liu, G.; Liashenko, A.; Piskorz, P.; Komaromi, I.; Gomperts, R.; Martin, R. L.; Fox, D. J.; Keith, T.; Al-Laham, M. A.; Peng, C. Y.; Nanayakkara, A.; Gonzalez, C.; Challacombe, M.; Gill, P. M. W.; Johnson, B.; Chen, W.; Wong, M. W.; Andres, J. L.; Gonzalez, C.; Head-Gordon, M.; Replogle, E. S.; Pople, J. A. *Gaussian 98*; Gaussian, Inc.: Pittsburgh, PA, 1998.
(25) Møller, C.; Plesset, M. S. *Phys. Rev.* **1934**, *46*, 618−622.
(26) Kuczera, K.; Wiorkiewicz, J. K.; Karplus, M. MOLVIB: Program for the Analysis of Molecular Vibrations; *CHARMM*; Harvard University, 1993.
(27) Brooks, B. R.; Bruccoleri, R. E.; Olafson, B. D.; States, D. J.; Swaminathan, S.; Karplus, M. *J. Comput. Chem.* **1983**, *4*, 187−217.
(28) Feller, S. E.; Venable, R. M.; Pastor, R. W. *Langmuir* **1997**, *13*, 6555−6561.
(29) Armen, R. S.; Uitto, O. D.; Feller, S. E. *Biophys. J.* **1998**, 75, 734−744.
(30) Feller, S. E.; MacKerell, A. D. *J. Phys. Chem.* **2000**, *104*, 7510−7515.
(31) Feller, S. E.; Yin, D.; Pastor, R. W.; MacKerell, J., A. D. *Biophys. J.* **1997**, *73*, 2269−2279.

Table 1. Geometries about the sp^2 and Central sp^3 Carbons for 1,4-Pentadiene and 2,5-Heptadiene from the MP2/6-31G** Ab Initio Calculations[a]

C=C–C–C	C=C	C–C	C=C–C	C–C–C	ΔE
		1,4-pentadiene			
116.4, 116.4	1.338	1.503	124.4	111.3	0.00
120.0, −120.0	1.337	1.503	124.3	111.7	0.72
−13.8, 115.5	1.338/1.338	1.508/1.498	125.1/124.3	113.9	0.48
		2,5-heptadiene			
111.3, 111.3	1.343	1.505	127.4	110.2	0.00
116.2, −116.2	1.343	1.505	127.3	110.6	0.40

[a] Angles in degrees, bond lengths in Å, and energies in kcal/mol. For the 1,4-pentadiene −13.8,115.5 structure the asymmetry of the conformational led to differences for the C−C bond and C=C−C angle; both values are reported.

as estimated from X-ray diffraction experiments on SDPC.[2] Initial coordinates of the DHA chain were generated by carrying out Langevin dynamics simulations of a single molecule and then combining randomly selected conformations onto lipids from a previous simulation of 1-palmitoyl-2-oleoyl-*sn*-glycero-3-phosphocholine.[29] The stearoyl chain conformations were generated by placing two additional carbon atoms (in the trans conformation) at the end of the palmitic acid.

The LJ potential was switched smoothly to zero over the region from 10 to 12 Å. Electrostatic interactions were included via the particle mesh Ewald summation.[32] All covalent bonds involving hydrogen were fixed at their equilibrium distances by using the SHAKE algorithm.[33] A time step of 2 fs was employed with a leapfrog Verlet integration scheme. A neighbor list, used for calculating the LJ potential and the real space portion of the Ewald sum, was kept to 12 Å and updated every 20 fs. A variant of the extended system formalism, the Langevin Piston algorithm,[34] was used to control the normal pressure. The temperature was maintained at 30 °C by means of a Hoover thermostat.[35] Coordinate sets were saved every 1 ps for subsequent analysis. Simulations were carried out by using eight processors on a Beowulf-type parallel computer, with each nanosecond of simulation taking approximately 5 days of wall time. The total simulation length was 16 ns, with the first nanosecond discarded as equilibration.

Results and Discussion

Quantum Mechanical Calculations. The properties of biological molecules in membranes are a balance between the intrinsic energetics of those molecules and environmental contributions. To evaluate the intrinsic energetic properties of polyunsaturated hydrocarbon chains, we undertook QM calculations on two model compounds that contain a 1,4-pentadienyl moiety. The 1,4-pentadiene (Figure 2, **C**) was selected as the simplest compound that can represent such a moiety, and 2,5-heptadiene (Figure 2, **D**) was chosen because of the terminal methyl groups that make it more representative of polyunsaturated lipids. For both compounds the global minimum is represented by a *skew*$^+$, *skew*$^+$ conformation of the two central single bonds (See Table 1). This is consistent with the crystal structures of various polyunsaturated fatty acids and with previous theoretical studies based on empirical force field models.[36−38]

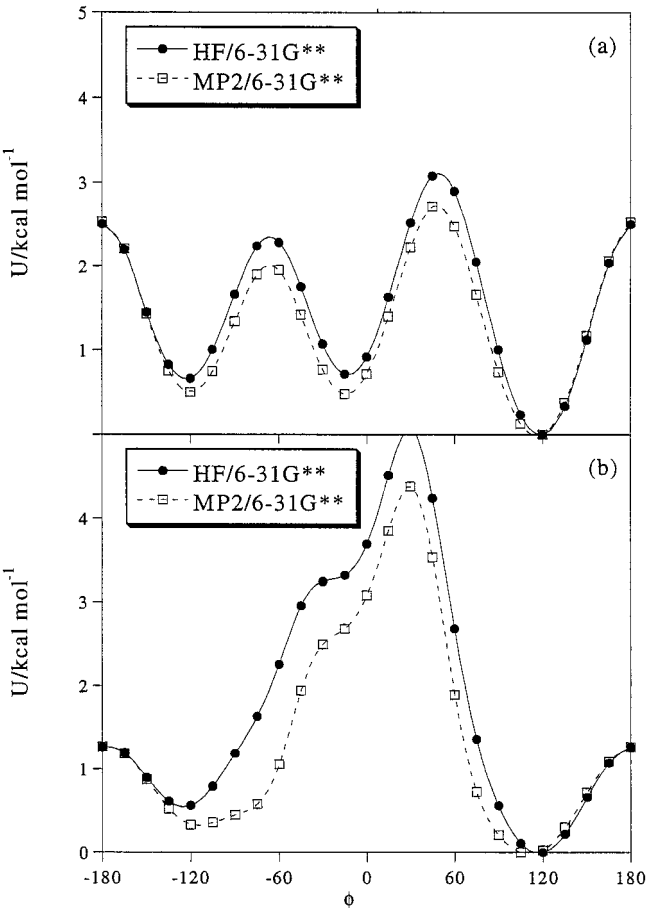

Figure 3. Potential energy surfaces for rotation about (A) the C2−C3−C4−C5 torsion in 1,4-pentadiene and the (B) C3−C4−C5−C6 torsion in 2,5-heptadiene for both HF/6-31G** (filled squares) and the MP2/6-31G** (filled circles) levels of theory. In both cases the second single bond surrounding the methyl group was constrained to 120°. Note that the anti (or trans) orientation corresponds to 180°.

To understand the conformational space that can be sampled in the vicinity of the minimum energy conformations in polyunsaturated hydrocarbons, QM torsional energy surfaces were obtained for one of the central single bonds in **C** and **D** with the second single bond constrained to 120° (Figure 3). In both cases there are minima in the vicinity of 120° (*skew*$^+$) and −120° (*skew*$^-$) with an additional minimum in the vicinity of 0° for **C**. This minimum is due to the C−C=C angle adjacent to the methylene being more open in the presence of the double bond, thereby reducing steric repulsion as compared to a saturated alkane. A corresponding minimum is not observed in **D** due to the presence of the terminal methyl groups on the cis double bonds. The relative energies of the *skew*$^+$, *skew*$^-$ minimum are 0.7 and 0.4 kcal/mol above the *skew*$^+$, *skew*$^+$ global minima for **C** and **D**, respectively (Table 1), values similar or lower than the relative energy of the gauche minimum in butane or hexane.[39] Notable are the broader minima in **D** as compared to **C**. Also of interest is the energy of the barrier between the *skew*$^+$ and *skew*$^-$ minima at 180°. In **C** the barrier is 2.5 kcal/mol while it is 1.3 kcal/mol in **D**. Thus, the presence of methyl groups in **D** leads to the 0° minimum being of high energy. However, the methyl groups lower the relative energy

(32) Essman, U.; Perera, L.; Berkowitz, M. L.; Darden, T.; Lee, H.; Pedersen, L. G. *J. Chem. Phys*. **1995**, *103*, 8577−8593.
(33) Ryckaert, J. P.; Ciccotti, G.; Berendsen, H. J. C. *J. Comput. Phys.* **1977**, *23*, 327−341.
(34) Feller, S. E.; Zhang, Y.; Pastor, R. W.; Brooks, B. R. *J. Chem. Phys.* **1995**, *103*, 4613−4621.
(35) Hoover, W. G. *Phys. Rev. A* **1985**, *31*, 1695−1697.
(36) Rabinovich, A. L.; Ripatti, P. O. *Biochim. Biophys. Acta* **1991**, *1085*, 53−62.
(37) Rich, M. *Biochim. Biophys. Acta* **1993**, *1178*, 87−96.
(38) Applegate, K. R.; Glomset, J. A. *J. Lipid. Res*. **1986**, *27*, 658.
(39) Smith, G. D.; Jaffe, R. L. *J. Phys. Chem.* **1996**, *100*, 18718−18724.

of the *skew*$^+$, *skew*$^-$ minimum and the barrier between the two minima.

The results for **D** differ substantially from data for saturated hydrocarbons, such as butane and hexane.[31] In saturated chains the anti orientation represents the global minimum while the gauche orientation occurs at 60° for the C−C−C−C torsion, with 120° representing a barrier. The relative energies of the gauche minima are approximately 0.5 kcal/mol. Thus, the energy of the second minimum in a polyunsaturated hydrocarbon is predicted to be lower than that in a saturated chain. Furthermore, the height of the barrier between minima in saturated hydrocarbons at 120° is approximately 3 kcal/mol,[39] which is significantly higher than the value of 1.3 kcal/mol found for the polyunsaturated chain based on **D**.

The QM calculations provide a basis for partial understanding of the altered properties of the polyunsaturated hydrocarbon chain compared to a saturated chain. The minimum at 120° appears to be the result of the presence of double bonds adjacent to the methylene group, leading to a more open C−C═C bond angle (Table 1). This also allows for the 0° local minimum in **C**. The terminal methyl groups in **D**, combined with the cis double bonds, result in a maximum at 0°, but how do they lead to the altered energetics in the angular range from 75° to 300°? Comparison of the Hartree−Fock and MP2 surfaces of **D** (Figure 3B) shows the energetics about the two minima to be lowered by the inclusion of electron correlation. This suggests that the lower energy of the *skew*$^+$, *skew*$^-$ conformation in **D** is the result of dispersion interactions involving the terminal methyls. However, the trans barrier heights in **D** are unaffected by the inclusion of electron correlation. Comparison of the internal geometries of **C** and **D** (Table 1) shows the double bonds in **D** to be slightly longer by 0.005 Å and the C−C═C angle to be larger by 3°. We suggest that these differences are responsible for the lower barrier at 180° in **D**. They appear to be the result of the presence of the methyl groups that alter the geometries about the double bonds.

Parametrization. Accurate MD simulations, as necessary to theoretically investigate environmental contributions to the properties of polyunsaturated lipids, require a well-optimized force field. Empirical force-field parameters for polyunsaturated fatty acids were developed to be consistent with the CHARMM27 lipid parameters for saturated[30,40] and monounsaturated chains.[31] The potential energy function in CHARMM has been described elsewhere,[23] and includes internal energy terms for bond lengths, bond angles, torsional angles, and improper torsional angles. The interactions between nonbonded atoms are described by Coulombic interactions between partial point charges on the atomic centers and a Lennard-Jones (LJ) 6-12 potential. For the present study the nonbonded parameters were transferred directly from the previously parametrized alkane[41] and alkene[31] CHARMM force fields. Initial internal parameters were obtained from those force fields and only those parameters unique to the present molecules were adjusted.

As a first step in the present study, the torsional parameters for the double bond were reinvestigated with 1-butene and 2-butene (**A** and **B** in Figure 2, respectively). This reanalysis was motivated by the availability of the present MP2 calculations (versus the previous Hartree−Fock calculation) for determining the surface for rotation about the double bond. Inclusion of electron correlation leads to a significant decrease in the barrier to rotation, from approximately 100 kcal/mol to 36 kcal/mol. Additionally, the potential energy surface of the single bond adjacent to the double bond and the vibrational spectra of compounds **A** and **B** were also reinvestigated with the higher level of theory. Presented in Tables 1 and 2 of the Supporting Information are the vibrational spectra of **A** and **B** for both the empirical and QM data. Overall, the agreement between the empirical and QM data is very good for the low-frequency modes concerning both the frequencies and the assignments. The largest discrepancies occur with the 2-butene wagging and deformation modes associated with the hydrogens attached to the double-bonded carbon (Table 2 of the Supporting Information, modes 5 and 6), with the empirical frequencies significantly lower than the QM values. However, since the corresponding modes in 1,4-pentadiene (**C**) were in good agreement with the QM data, further adjustments were not performed. A comparison of the energy surfaces for rotation in **A** and **B** is shown in Figure 1 of the Supporting Information. For 1-butene (**A**) the empirical and QM surfaces are in excellent agreement (Supporting Information, Figure 1A). With 2-butene (**B**) it was necessary to sacrifice the empirical barrier height to allow for the lower energy region of the surface (Supporting Information, Figure 1B) to be reproduced. This choice was motivated by the desire to accurately model the regions of lower energy that are sampled in a typical MD simulations (the high-energy regions, though lower than the QM energies, will still be forbidden in room temperature MD simulations). In both the QM (not shown) and empirical 2-butene energy surfaces there are discontinuities in the vicinity of the barrier. This is the result of "jumping" between conformations by the hydrogens that are covalently bound to the sp^2 carbons as the barrier is crossed. Again, due to the high energy levels at which these events occur it may be assumed that they will be absent in MD simulations.

The next optimization efforts focused on the two single bonds and the methylene group between double bonds in polyunsaturated lipids with 1,4-pentadiene (**C**) and 2,5-heptadiene (**D**) as model compounds. Geometric information for these compounds is shown in Table 3 of the Supporting Information. Included in the table are results from a survey of 1,4-pentadienyl moieties in the Cambridge Structural Database.[42] This search identified a total of seven 1,4-pentadienyl moieties from which the statistics in Table 3 were obtained. In general the empirical data are in good agreement with the QM data for the bond lengths and angles. With respect to the survey data, the empirical bond lengths are slightly too long, resulting in better agreement with the QM data, while the empirical bond angles are close to the survey data. Concerning the minimized dihedral angles for compounds **C** and **D**, the agreement between the QM and empirical results is good, with the exception of the empirical *skew*$^+$, *skew*$^-$ conformation of **D**. The CHARMM *skew*$^+$ dihedral angle is significantly lower than the QM value. This difference was necessary to fit the torsional energy surface for **D** (see below). Force constants for the 1,4-pentadienyl moiety

(40) Schlenkrich, M.; Brickmann, J.; MacKerell, A. D., Jr.; Karplus, M. In *Biological Membranes: A Molecular Perspective from Computation and Experiment*; Merz, K. M., Roux, B., Eds.; Birkhaüser: Boston, 1996; pp 31−81.
(41) Yin, D.; MacKerell, A. D., Jr. *J. Comput. Chem.* **1998**, *19*, 334−348.
(42) Allen, F. H.; Bellard, S.; Brice, M. D.; Cartwright, B. A.; Doubleday, A.; Higgs, H.; Hummelink, T.; Hummelink-Peters, B. G.; Kennard, O.; Motherwell, W. D. S.; Rodgers, J. R.; Watson, D. G. *Acta Crystallogr.* **1979**, *B35*, 2331−2339.

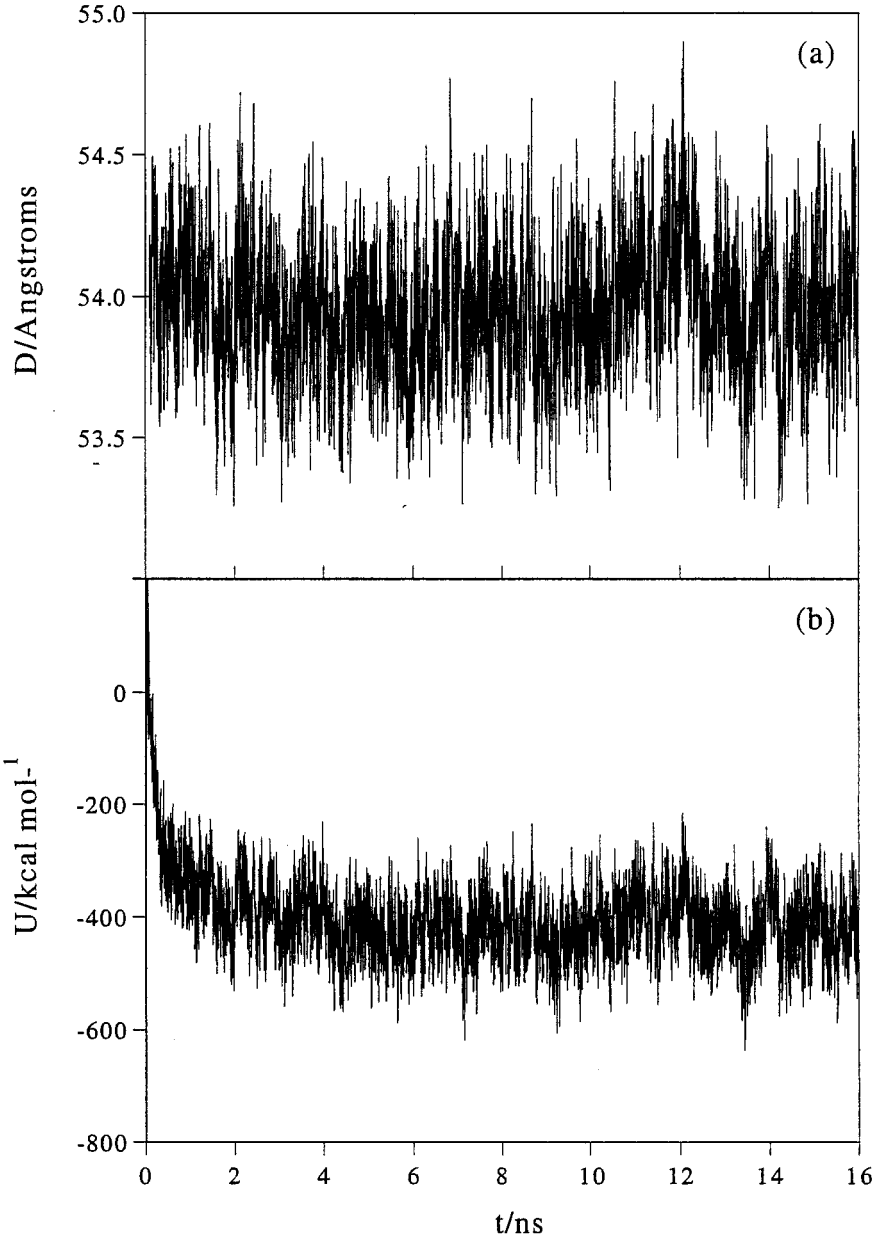

Figure 4. (A) Bilayer repeat spacing for the simulation of SDPC as a function of time. The experimental value is 54.0 Å. (B) Internal energy as a function of time. The first nanosecond of simulation was discarded as equilibration and not used in the analyses reported here.

were optimized to reproduce vibrational spectra of **C** and torsional energy surfaces for **C** and **D**. Presented in Table 4 of the Supporting Information is a comparison of the empirical and QM vibrational spectra of **C**. Inspection of this table shows good agreement between the force field and QM results both with respect to frequencies and assignments. This level of agreement indicates that the molecular distortions that occur during MD simulations will be adequately represented by the force field.

Final optimization of the torsional parameters for the 1,4-pentadienyl moiety was based on reproduction of potential energy surfaces for **C** and **D**. Figure 2 of the Supporting Information shows surfaces for **C** with the second single bond constrained to 120° or 0°. For the 120° surface (Supporting Information Figure 2A) the agreement is excellent with respect to both location of minima and energetics. In the second surface, with the second single bond constrained to 0° the agreement in the low-energy regions is good, while the energies of the higher energy regions are underestimated by the force field. A similar effect was observed for **D** with the second single bond constrained to 120°, as shown in the Supporting Information (Figure 3A) In both cases agreement in the high-energy regions was sacrificed in order to better reproduce the energetics of the low-energy regions. As will be shown in the analysis of the MD simulations, the high-energy region in the vicinity of 0° is rarely sampled (Figure 5), indicating that the sacrifice does not lead to improper behavior. A second energy surface for **D** was obtained with the neighboring dihedral angle constrained to 180° (Supporting Information, Figure 3B) resulting in good agreement between the QM and MM surfaces. Finally, energy surfaces for **D** were obtained with the double bonds in the trans orientation and the second single bond constrained to 120° (Supporting Information, Figure 3C). Initial calculations (not shown) using the dihedral parameters optimized for cis double

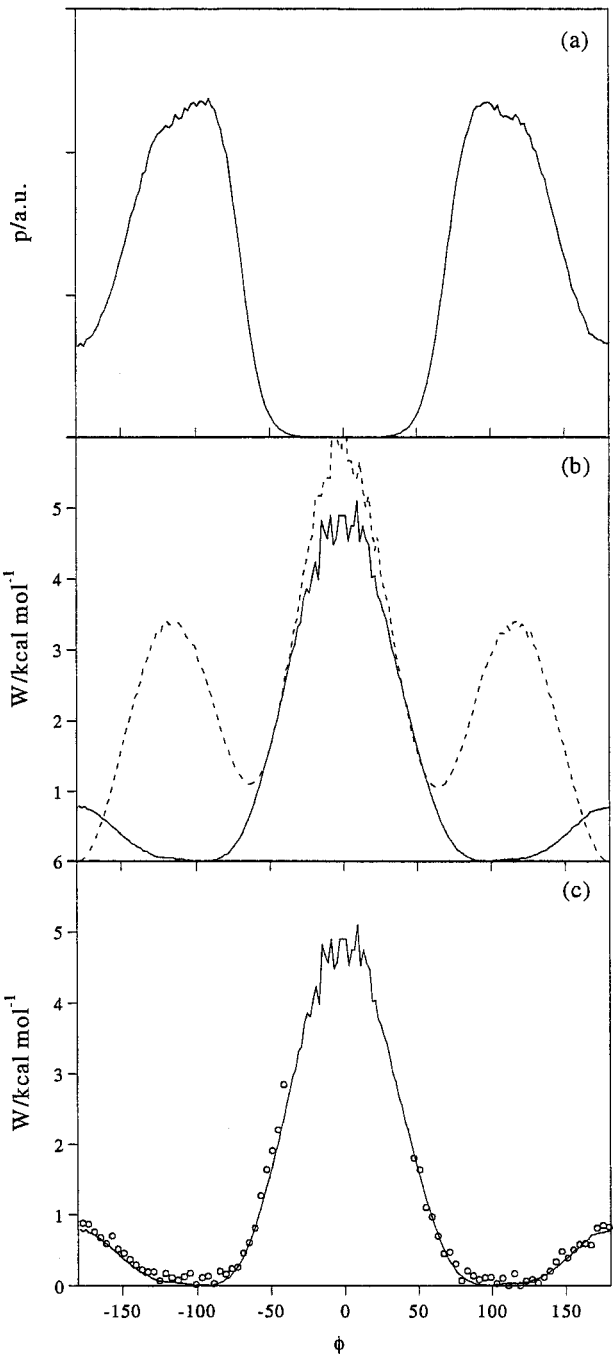

Figure 5. (A) Probability distribution for the C10−C11−C12−C13 and C11−C12−C13−C14 dihedral angles in the DHA chain. (B) Potential of mean force for rotation about the dihedral angles in (A) (solid), and for rotation about the corresponding dihedrals in the saturated sn1 chain (dashed). (C) Potential of mean force for the C10−C11−C12−C13 and C11−C12−C13−C14 dihedral angles in the polyunsaturated sn2 chain (solid), and for rotation about the corresponding dihedrals in a gas-phase simulation of an isolated 2,5-heptadiene molecule (symbols). Note that the anti (or trans) orientation corresponds to 180°.

bonds yielded poor agreement with the QM data. Accordingly, a second set of dihedral parameters for the C═C−C−C torsion were optimized to reproduce the trans double bond surface, resulting in good agreement between the empirical and QM data. Thus, to properly treat polyunsaturated lipids with trans double bonds, versus the cis double bonds that occur under physiological conditions, a different set of dihedral angle parameters must be employed. Simulations where both cis and trans double bonds are present require the assignment of unique atom types to the trans double bonds so the appropriate parameters can be applied.

Overall, the optimized parameters for polyunsaturated moieties in lipids reproduce both experimental and QM data for geometries, vibrational spectra, and energetics. Although certain limitations in the energetic properties are evident at the model compound level, these do not result in aberrant behavior in the MD simulations (see below). A list of the new parameters that may be used to supplement the CHARMM27 all-atom force field for lipids is included in Table 5 of the Supporting Information.

Bilayer Simulation. The SDPC bilayer simulation was carried out at a fixed surface area corresponding to the dimensions determined experimentally at a temperature of 30 °C and a water/lipid ratio of 15.1. The experimentally measured bilayer repeat spacing, D, is 54.0 Å under these conditions.[2] Figure 4 shows the time evolution of the bilayer repeat spacing and the system energy during the simulation, demonstrating that the system volume is reproduced to within less than 0.1% (D = 53.96 Å) and that the simulation is stable on the multinanosecond time scale. The relaxation of the system's internal energy during the first nanosecond of the simulation suggests that brief simulations, of the order of 1 ns, will be strongly affected by the choice of initial conditions.

To characterize the torsional states of the DHA chain, probability distributions, $p(\phi)$, for rotation about each of the vinyl−methylene bonds were constructed from the simulation trajectory. The probability distributions were subsequently converted into potentials of mean force, $W(\phi) = -RT \ln p(\phi) + C$, to quantify rotational barriers. Results for the average of the C10−C11−C12−C13 and C11−C12−C13−C14 torsions, which are typical of all the distributions, are given in Figure 5 (probability in Figure 5A, potential of mean force in Figure 5B—solid line). The extremely low barrier to rotation at 180° (less than 1 kcal/mol) and broad potential energy minima indicate a very flexible chain. For comparison, data from the corresponding dihedrals of the saturated sn-1 chain are given as a dashed line in Figure 5b, showing well-defined torsional states separated by barriers of several kilocalories/mole. To quantify any effects of the lipid bilayer environment on the vinyl−methylene torsion, simulations of 2,5-heptadiene in the gas and neat liquid states were carried out and the potentials of mean force for rotation about the central torsions calculated. Sampling of the torsional space was very similar in all three cases, with results for the DHA and gas-phase heptadiene given in Figure 5C.

Partially assigned C−H bond order parameters of perdeuterated docosahexaenoic acid were obtained by ^{13}C NMR.[3] Additionally, DHA order parameters were obtained by ^{2}H NMR after incorporation of perdeuterated DHA (as free fatty acid) into a 1-stearoyl-2-oleoyl-*sn*-glycero-3-phosphocholine bilayer (details of perdeuterated DHA synthesis and NMR data analysis have been submitted for publication to the Journal of Lipid Research). The order parameter, S_{CD}, can be measured experimentally from the quadrupolar splitting, $\Delta\nu_Q$, in an axially averaged line shape,

$$\Delta\nu_Q = \frac{3}{4}\left(\frac{e^2qQ}{h}\right)S_{CD} \qquad (1)$$

where the term in parentheses is the quadrupolar coupling

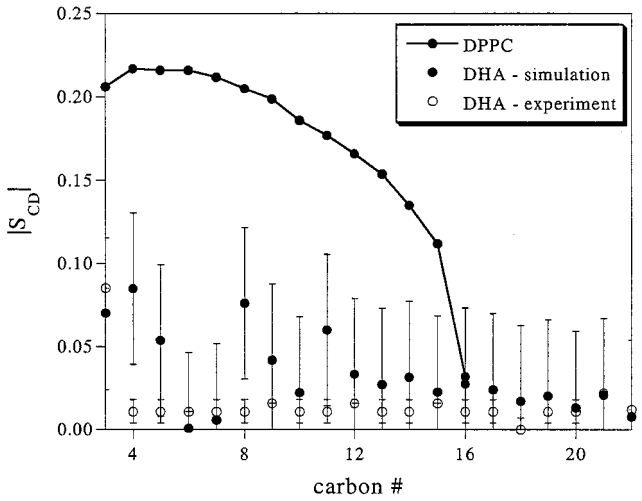

Figure 6. Deuterium order parameter profiles. The points are the results for the DHA chain (experimental = open symbols, simulation = solid symbols). Experimental error bars give the range of order parameters observed for unassigned resonances. Simulation error bars give the standard deviation calculated from among the 72 chains. Filled symbols, connected by a solid line, give the results of a saturated sn2 chain (DPPC from ref 23) for comparison.

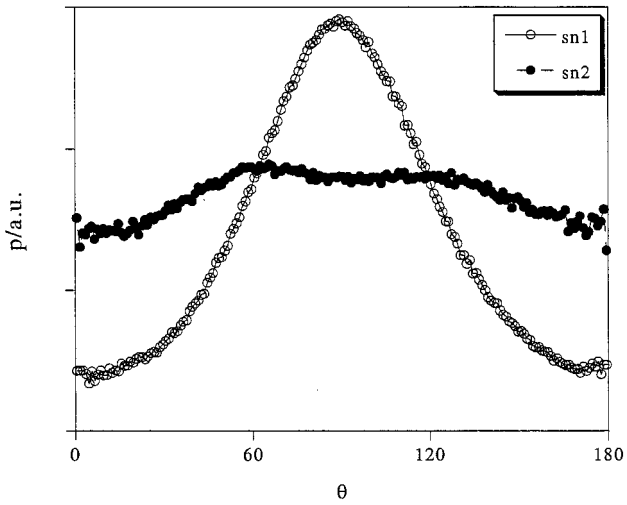

Figure 7. Probability distribution for the angle, θ, between the CH vector at carbon position 9 and the bilayer normal. The open and solid symbols give the results for the saturated and polyunsaturated chains, respectively.

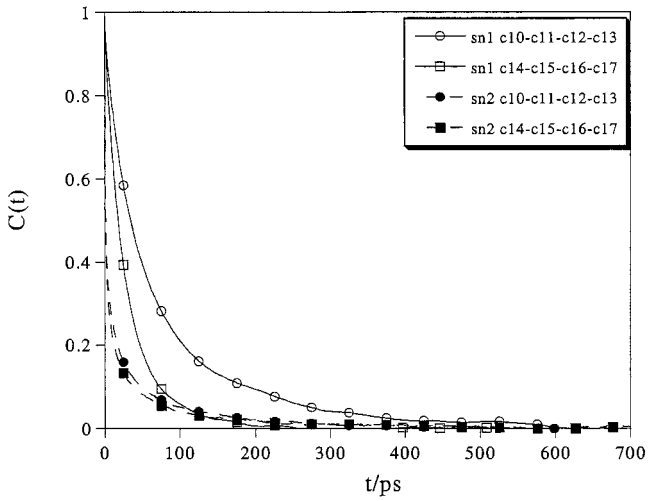

Figure 8. Autocorrelation functions for dihedral angles in the saturated (open symbols) and polyunsaturated (solid symbols) chains of the SDPC bilayer.

constant. From the simulation, S_{CD} is calculated from

$$S_{CD} = \left\langle \frac{3}{2}\cos^2\theta - \frac{1}{2} \right\rangle \tag{2}$$

where θ is the angle between the C−H bond vector and the bilayer normal and the brackets denote an averaging over time and over all lipids. The calculated deuterium order parameter profile of the polyunsaturated sn2 chain is presented in Figure 6 along with the corresponding experimental values.[3] The dramatically different conformational properties of the saturated and docosahexaenoic acid chains lead to large variation in deuterium order parameter values. The lack of order in the polyunsaturated chain is striking and reproduces reasonably well the experimental observations, although the experimental order parameters appear to be even lower than those calculated from simulation. Possible origins of this small discrepancy are the use of free fatty acid for the experimental order parameter determination and the relatively high order parameters of the simulation initial conditions. For comparison purposes, values of a saturated palmitic acid chain in the sn-2 position are given from an earlier simulation, emphasizing the dramatic effect of unsaturation on chain order. Essentially every DHA chain position has a level of disorder similar to the terminal methyl group of DPPC.

Low values of the deuterium order parameters can result from one of two mechanisms. In the preceding paragraph it was implicitly assumed that the low order parameters observed along the DHA chain are the result of a truly disordered chain where the averaging inherent in eq 2 was over a nearly uniform distribution of θ values. An alternative explanation is that the chains are not necessarily disordered, but rather take on rigid conformations such that θ is close to the "magic angle" of 54.7°. To investigate this possibility, the probability distribution for the angle between the C−H vectors at position 9 of the fatty acid chains with the bilayer normal has been calculated and is plotted in Figure 7. Clearly, the differences in deuterium order parameters that are observed between saturated and polyunsaturated chains are the results of conformational averaging that sample vastly different ranges of θ values. This distinction is critical in the interpretation of deuterium NMR order parameter data.

The low barriers to torsional rotation suggest that the chains will rapidly interconvert between a large number of conformational states. To describe the time scale of these internal motions, we have calculated the normalized dihedral angle autocorrelation function,

$$\cos(\phi(t))\cos(\phi(t+t')) \tag{3}$$

for various positions along the fatty acid chains. The results are given in Figure 8. Correlation times for the dihedral angles in the middle of the polyunsaturated chain were found to be ∼20 ps, from integration of the correlation functions in Figure 8. This can be compared with values of 70 and 30 ps for the corresponding positions in the saturated chains. In addition to the significantly shorter correlation times, the polyunsaturated chain does not exhibit the gradient of fluidity seen in the saturated chain, with little dependence of the correlation time on position within the chain.

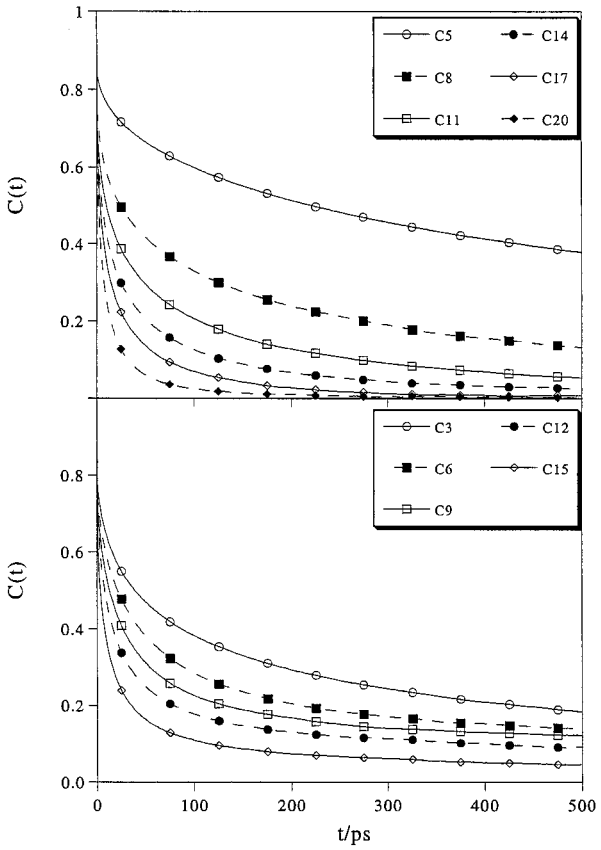

Figure 9. Reorientational correlation functions of the CH vectors at various positions along the saturated (lower frame) and polyunsaturated (upper frame) o SDPC bilayer.

The dynamics of chain segments have been studied experimentally through measurements of the ^{13}C spin−lattice (T_1) relaxation rates.[3] These rates can be related to the lipid dynamics through the Fourier transform of the reorientational correlation function

$$C(t) = \langle P_2(\mu(0)\,\mu(t))\rangle \tag{4}$$

where P_2 is the second-order Legendre function and μ is the vector of unit length directed along the C−H bond vector. The Fourier transform of the correlation function defined by eq 4 gives the spectral density

$$J(\omega) = \int_0^\infty C(t)\cos(\omega t)\,\mathrm{d}t \tag{5}$$

which determines the relaxation time through

$$\frac{1}{nT_1} = \frac{4\pi}{10}\left(\frac{\mu_0\mu_H\mu_C}{\pi\hbar r^3}\right)^2 \times (J(\omega_C - \omega_H) + 3J(\omega_C) + 6J(\omega_C + \omega_H)) \tag{6}$$

where ω_C and ω_H are the carbon and hydrogen Larmor frequencies, respectively. The reorientational correlation functions for C−H vectors at the double bond positions of the DHA chain are given in Figure 9 along with selected positions along the saturated chain for comparison. In the mid and upper sections of the chains, the results for the saturated sn-1 and polyunsaturated sn-2 chains are similar with the exception of enhanced short time relaxation in the DHA chain. The faster relaxation in the DHA chain is likely due to the extremely rapid dihedral

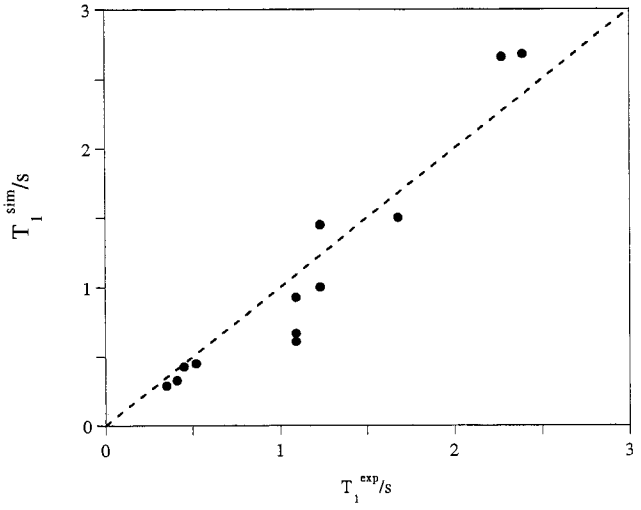

Figure 10. A comparison of T_1 relaxation times from simulation and experiment.

transitions described in Figure 8. In contrast to DHA dihedral angle autocorrelation functions, which showed little dependence on chain position, the reorientational correlation functions of the DHA chain show significantly faster reorientation near the terminal methyl group, suggesting concerted motions involving several methylene groups occur more rapidly near the end of the chain. These correlation functions are consistent with the experimentally measured T_1 values, where vinyl resonances produced relaxation times in the range 0.35−2.39 s at a ^{13}C resonance frequency of 125.72 MHz.[3] After Fourier transformation of the simulation correlation functions, T_1 values for the vinyl positions were calculated and are compared with the experimental values in Figure 10. The vinyl resonances were partially assigned by their chemical shift. Where the assignment was ambiguous, experimental data are presented assuming that the T_1 values increase moving down the chain (the ordering observed in the simulation and in previous experiments on saturated chains). The agreement with experiment is very good, reproducing the range of values covering 1 order of magnitude.

The picture that emerges from the QM calculations on model compounds, the MD simulation of a polyunsaturated bilayer, and the NMR experimental results discussed above is of extremely flexible chain segments that allow rapid interconversion between conformations. It has been suggested, based on a combined NMR and X-ray scattering study of bilayer area compressibility, that in SDPC this flexibility leads to differences in chain compressibility.[2] From the simulation this issue may be addressed, at least qualitatively, by analyzing the fluctuations of the instantaneous surface areas per fatty acid chain. The method of Voronoi polyhedra was employed where polygons are constructed in the plane of the membrane such that they inscribe the region of space that is closest to the center of mass of each chain.[43,44] In this way, the surface area requirement of each chain is determined. The probability distribution for single chain areas is given in Figure 11 for the saturated and polyunsaturated chains. The DHA chain has a greater mean and broader distribution of surface areas, in agreement with the hypothesis of greater compressibility in polyunsaturates. Furthermore, calculations of the compressibility modulus, from

(43) Shinoda, W.; Okazaki, S. *J. Chem. Phys.* **1998**, *109*, 1517.
(44) Feller, S. E.; Pastor, R. W. *J. Chem. Phys.* **1999**, *111*, 1281.

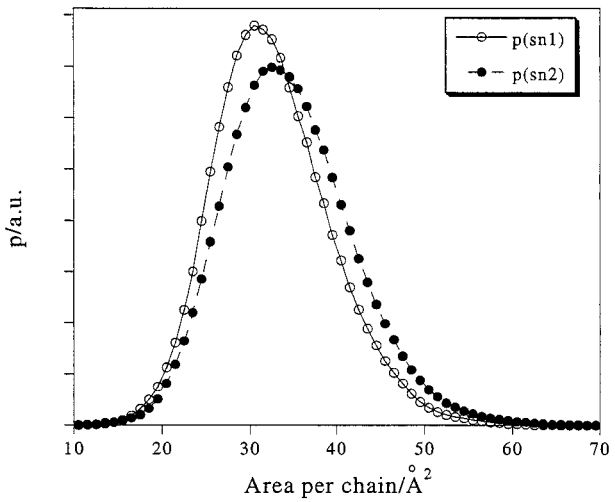

Figure 11. The distribution of single-chain surface areas as calculated from the simulation trajectory using the Voronoi polyhedra method. The saturated sn1 chain is given as a solid line and the polyunsaturated sn2 chain is shown as a dashed line.

fluctuations in the instantaneous area per molecule, show a reduction of ~20% compared to our previous simulations of saturated lipids.[44]

Conclusions

Results of the quantum mechanical calculations clearly demonstrate that the presence of polyunsaturation in a hydrocarbon chain intrinsically increases the amount of conformational space accessible about the central methylene group as compared to saturated hydrocarbon chains. When these data were incorporated into an empirical energy function suitable for use in molecular dynamics simulation, the result was an extremely disordered membrane with rapid interconversion among torsional states. The enumeration of these torsional states is complicated by the broad dihedral energy minima characteristic of this system; however, cluster analysis of the 10 rotatable dihedral angles between vinyl groups was able to produce approximately 100 families of high-probability conformers. Four such conformers are presented in Figure 12 that illustrate the great diversity of DHA chain conformations and help to visualize the various results described in the preceding section.

The present calculations support a model of extreme flexibility for the DHA chain, as opposed to one rigid structure or a few selected structures. These observations are consistent with the increased mobility observed in experiments probing C−H bond order parameters, ^{13}C spin−lattice relaxation times, and area compressibility moduli. Our results are also largely consistent with previous modeling studies on DHA and related systems.[36−38,45] Approaches utilizing molecular mechanics,[38] quenched MD/energy minimization[37] and Monte Carlo simulations[36] of polyunsaturated fatty acid chains, and a recent MD simulation of a fully hydrated SDPC bilayer[45] all produced DHA conformations that differ markedly from saturated chains. However, the present study is, to our knowledge, the first to employ a force field based on high-level QM calculations of the pentadienyl moiety that is the fundamental unit of the DHA chain. Additionally, the production run of the present simulations is more than an order of magnitude longer than any previous works, allowing a rigorous test of the potential energy parameters. The availability of a high-quality force field provided by this work provides the opportunity to investigate a number of properties of polyunsaturated lipids and to compare, at atomic-level detail, differences between polyunsaturated, monounsaturated, and saturated fatty acids.

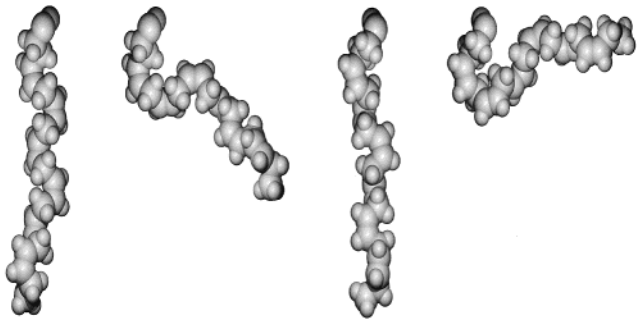

Figure 12. Representative conformations of the DHA chain generated in the MD simulation.

Acknowledgment. We thank the National Institutes of Health (GM5150-01 to A.D.M. Jr). and the National Science Foundation (MCB-0091508 to S.E.F.) for financial support.

Supporting Information Available: Experimental data (PDF). This material is available free of charge via the Internet at http://pubs.acs.org.

JA0118340

(45) Said, L.; Klein, M. L. *Biophys. J.* **2001**, *82*, 204.